Paf1c defects challenge the robustness of flower meristem termination in *Arabidopsis thaliana*

Kateryna Fal*,[1], Matthieu Cortes*,[1], Mengying Liu[1], Sam Collaudin[1], Pradeep Das[1], Olivier Hamant[1,#], Christophe Trehin[1,#]

1 Laboratoire de Reproduction et Développement des Plantes, Université de Lyon, UCB Lyon 1, ENS de Lyon, INRA, CNRS, 46 Allée d'Italie, 69364 Lyon Cedex 07, France

Contacts : christophe.trehin@ens-lyon.fr, olivier.hamant@ens-lyon.fr

* Equal contributions

Summary statement

Using a mutant with increased transcriptional noise, we reveal that stem cell maintenance is not as robust as anticipated in plants, even leading to major defects in essential developmental processes such as flower indeterminacy.

ABSTRACT

While accumulating evidence suggests that gene regulation is highly stochastic, genetic screens successfully uncovered master developmental regulators, questioning the relationship between transcriptional noise and intrinsic robustness of development. Here we use the *Arabidopsis* Paf1c mutant *vip3*, which is impaired in several RNA Pol II-dependent transcriptional processes, to identify developmental modules that are more or less resilient to large-scale genetic perturbations. We find that the control of flower termination is not as robust as classically pictured. In Angiosperms, the floral female organs, called carpels, display determinate growth: their development requires the arrest of stem cell maintenance. In *vip3* mutant flowers, carpels displayed a highly variable morphology, with different degrees of indeterminacy defects up to wild-type size inflorescence emerging from carpels. This phenotype was associated with a variable expression of two key regulators of flower termination and stem cell maintenance in flowers, *WUSCHEL* and *AGAMOUS*. This phenotype was also highly dependent on growth conditions. Altogether, these results highlight the surprisingly plastic nature of stem cell maintenance in plants, and its Paf1c dependence.

Keywords: Floral determinacy, transcriptional noise, Paf1 complex, *WUSCHEL*, *AGAMOUS*, carpel, stem cell, variability, developmental robustness

INTRODUCTION

Developmental robustness is ambivalent: patterns of growth must be reproducible, as body plans are usually comparable within individuals of given species; they also must be plastic to adapt to external and internal changes and fluctuations. In other words, developmental robustness entails a balance between homeostatic mechanisms that ensure that many phenotypes are robust to genetic and environmental variations, and variability promotion to trigger alternative developmental pathways to face genetic and environmental variations. This balance is also a variable, as the ratio between reproducibility and variability promotion can shift as development goes on (see e.g. (Tsugawa et al., 2017)).

Among the factors behind developmental robustness, transcriptional noise can contribute to specific differentiation pathways in various tissues (Mason et al., 2014)(Mantsoki et al., 2016)(Alemu et al., 2014)(Padovan-Merhar and Raj, 2013)(Sprinzak et al., 2010). Besides, the maintenance of stem cells may rely on the relative inefficiency of the transcriptional and translational machinery that maintains the stem cell in an indeterminate state (Momiji and Monk, 2009). Interestingly, variability of gene expression can account for reduced penetrance (Raj et al., 2010). In plants, the contribution of gene expression variability to plant developmental robustness and plasticity remains poorly documented. Gene expression variability has mainly been assessed during responses to external or internal stimuli (Waters et al., 2017)(Xu et al., 2016)(Wang et al., 2011) and only more recently as an internal input to support developmental plasticity at tissue level (Meyer et al., 2017).

Although the exact mechanisms behind transcriptional noise remain to be uncovered, relevant molecular factors are starting be identified. For instance, the variability of gene expression in mammals relies on several features of the gene itself spanning from its genomic structure and regulation to its interacting network (Alemu et al., 2014). Interestingly, the RNA polymerase II-associated factor 1 complex (Paf1c) seems to play a key role in this process. Mutations in Paf1c subunits increase gene expression noise in yeast (Ansel et al., 2008)(Richard and Yvert, 2014). This effect not only relies on the functional interaction with RNA PolII, but also on a larger spectrum of activities. In plants, Paf1c has indeed been shown to influence gene expression through regulation of transcription (Oh et al., 2004)(Antosz et al., 2017), as well as chromatin modifications (He et al., 2004)(Oh et al., 2008). In mammals, Paf1c also restrains the activation of enhancers, and thus hinders the release of paused RNA PolII, adding another layer of control of gene expression variability (Chen et al., 2017). In principle,

mutants in Paf1c subunits thus offer the ideal context to analyze the role of transcriptional noise in development.

One of the Paf1c components, *VERNALIZATION INDEPENDENCE 3* (*VIP3*), was initially shown to control flowering time (Zhang et al., 2003). Recently, *vip3* mutants were found to exhibit variable phyllotactic patterns: *vip3* mutants exhibit a divergence angle of 137° between each organ initiation at the shoot apex on average, as in the wild type, but the standard deviation of that angle is increased in the mutant (Fal et al., 2017). Because no other mutant exhibits such a phenotype, this finding suggests that Paf1c-dependent transcriptional control may be important for developmental robustness as a whole. Here we investigate whether flower termination, a developmental process that is both central to plant reproduction and very reproducible, may also depend on Paf1c.

Flowers are produced by the shoot apical meristem (SAM), which hosts a pool of pluripotent stem cells. This explains why the SAM at the tip of an inflorescence stem produces an indeterminate number of flowers (Besnard et al., 2011). The young flower also exhibit a meristematic activity early on, but in contrast to the SAM, it produces a determinate number of organs (4 sepals, 4 petals, 6 stamens and 2 carpels in *Arabidopsis thaliana*). This implies that the maintenance of the stem cell pool is stopped as the flower matures. Two decades of molecular genetics have demonstrated that stem cell homeostasis relies on a negative feedback loop involving the WUSCHEL (WUS) and CLAVATA (CLV) factors (Somssich et al., 2016). *WUS* encodes a homeodomain transcription factor and is expressed deep inside the SAM, in the organizing center (Mayer et al., 1998). The WUS protein moves to the central zone to promote both stem cell identity and *CLV3* expression (Yadav et al., 2011) (Daum et al., 2014). The CLV3 ligand diffuses in the upper part of the meristem and triggers the CLV-CORYNE pathway that, together with RPK2, restricts the *WUS* expression to the organizing center (Lenhard and Laux, 2003)(Rojo, 2002)(Kinoshita et al., 2010)(Brand, 2000)(Schoof et al., 2000)(Muller et al., 2008). More recently, the *ERECTA* receptor kinase (*ER*) and most of the *HD-ZIPIII* genes have been shown to regulate meristem size and stem cell homeostasis through different pathways and in parallel to the CLV pathway (Green et al., 2005)(Prigge et al., 2005)(Williams, 2005)(Mandel et al., 2014)(Mandel et al., 2016). All these genetic pathways, together with additional layers of control (e.g. transcriptional regulators (HAM, Zhou et al., 2018; ULT1/2, (Carles, 2005)(Monfared et al., 2013), chromatin regulators (FAS1/2, (Kaya et al., 2001); SYD, (Kwon, 2005)), cytokinins (Leibfried et al., 2005)(Gordon et al., 2009)), meristem geometry (Gruel et al., 2016), and environmental

factors (Pfeiffer et al., 2017)), robustly maintain and confine the stem cell niche before flowers are produced.

The flower initially inherits the potential of indeterminacy from the SAM: the maintenance of stem cell in the center of the flower relies on the same WUS/CLV regulatory loop (Schoof et al., 2000). Floral termination coincides with the end of *WUS* expression once carpels have been produced, at stage 6 (according to (Smyth et al., 1990)) in *Arabidopsis thaliana* (Mayer et al., 1998). AGAMOUS (AG), a MADS box transcription factor (Yanofsky et al., 1990), has been shown to be a key regulator in this process and triggers flower meristem termination, by repressing *WUS* expression (Lohmann et al., 2001)(Lenhard et al., 2001). This repression by AG can be direct, by recruiting PcG factors and promoting a chromatin loop that blocks the recruitment of RNA polymerase II at the *WUS* locus (Liu et al., 2011)(Guo et al., 2018) but also indirect through the activation of KNUCKLES (C2H2 Zn-finger transcription factor (Sun et al., 2009)). KNU, (i) is recruited to the *WUS* locus by MINI ZINC FINGER2 to form a complex together with HISTONE DEACETYLASE-like HDA19 and TOPLESS that in turn inhibits *WUS* expression (Sun et al., 2009)(Sun et al., 2014)(Bollier et al., 2018), and (ii) directly binds the *WUS* locus to cause eviction of SYD and to subsequently recruit PcG factors to silence *WUS* (Sun et al., 2019). Consistently, most mutants showing flower termination defects also show a transient reduction of *AG* expression in the center of the flower (Clark et al., 1993)(Fletcher, 2001)(Prunet et al., 2008)(Das et al., 2009)(Maier et al., 2009). Interestingly, recent data report how AG also influences auxin and cytokinin biosynthesis during flower meristem termination process (Yamaguchi et al., 2018)(Zhang et al., 2018). Similarly, the expression of a miR172-insentive version of *APETALA2* (*AP2*) results in a decrease of *AG* expression and in the development of supernumerary organs in the center of the flower (Zhao et al., 2007). AP2 may also promote floral stem cell maintenance by counteracting *AG* function (Zhao et al., 2007)(Liu et al., 2014)(Huang et al., 2017). Interestingly, mutations in many genes reported above as involved in the control of stem cell homeostasis in the SAM (including *CLV*, *ULT*, *ER*, *HD-ZipIII*) results in FM indeterminacy, this phenotype being often related to defect in AG expression. It seems therefore that *AG* expression is a good integrator and proxy for the final developmental decision to switch from an indeterminate to a determinate flower. Although single mutants have revealed that this process can be impaired, the contribution of transcriptional noise to the robustness of flower termination remains unknown.

We report here that mutations in Paf1c can result in a loss of floral determinacy. Such a phenotype is due to the maintenance of stem cells in the center of the flower beyond stage 6 that results of a global decrease of *AG* expression in the center of the flower. Importantly, this phenotype is not fully penetrant, with flowers exhibiting subtle defects to fully indeterminate phenotypes even on the same individual plant. This phenotype also depends on environmental conditions suggesting that Paf1c integrates both developmental and environmental cues to reduce *AG* expression variability during flower development and hinder floral indeterminacy.

RESULTS

vip3 mutants exhibit strong and variable flower indeterminacy

vip3 mutants have previously been reported to display a number of growth defects (Zhang et al., 2003)(Takagi and Ueguchi, 2012)(Dorcey et al., 2012)(Fal et al., 2017). When *vip3* mutants were grown for 3 weeks under short day conditions (21°C), and then transferred to continuous light (16°C), we observed a dramatic loss of floral indeterminacy such that, in some *vip3* plants, a wild-type sized inflorescence would grow out of a carpel (Figs. 1A,B, Fig. S1, N>30 plants). Whereas this phenotype was observed in both *vip3-1* and *vip3-2* alleles (Fig. 1C), in these growth conditions, silique development in the wild type remained entirely unaffected (Fig. 1A,C, N>30 plants).

To check whether this phenotype depends on either the temperature or day length shift, we next compared the *vip3-1* phenotype in different growth conditions. Plants grown in similar light conditions but at 21°C in continuous light instead of 16°C displayed a similar phenotype (Fig. S2, N=32 plants). We could also see the indeterminacy phenotype when *vip3-1* was constantly grown under short day conditions (Fig. S3A, N=9 plants) and under short then long day conditions (Fig. S3B, N=22 plants). When grown in long days, the *vip3* mutant was much smaller, with shorter stems, and exhibited a large number of aborted siliques without indeterminacy (Fig. S3C, N=36 plants). Therefore, floral termination defects in *vip3* only require short day conditions and no other specific growth conditions. Note that, except when

plants are grown exclusively under long day conditions resulting in sterile siliques (Fig. S3C), the *vip3* mutant was able to produce seeds but with a very low rate (Fig. S4).

The extent of the floral indeterminacy defects in *vip3* depended on growth conditions: the *vip3* phenotype was the most affected in short day and in short day then continuous light (16°C or 21°C) conditions and appeared to be the closest to a full reversal of floral identity reported in the literature. Note that we observed similar phenotypic defects in *vip6*, a mutant for another component of the Paf1 complex (Fig. S3D, N=19 plants). Such data further confirm that flower phenotypes result from defect in the Paf1-C complex and not in the Exome complex involved in mRNA turnover and whom VIP3 is also part of (SKI8, Dorcey et al., 2012)

Last, the *vip3* indeterminacy phenotype was also highly variable within a single plant (Fig. 1A, Fig. S2A). In comparison to the wild type, the phenotype ranged from short and bumpy siliques to completely open siliques containing a full inflorescence. With respect to the position of the siliques along the inflorescence stem, we found that early siliques were very often the most affected, although even the last siliques occasionally exhibited a strong phenotype too (Fig. 1C, Fig. S2B).

Supernumerary organs develop from the center of the floral meristem

Except for branching meristem that develop from bract axils in species with a dichasium inflorescence (Claßen-Bockhoff and Bull-Hereñu, 2013) or from sepal axils in *ap1* mutants that lack petals and have sepals displaying bract like features (Irish and Sussex, 1990)(Mandel et al., 1992), there are two ways in which flower indeterminacy may occur: either the flower maintains its stems cells after stage 6 (Prunet et al., 2009), or ovules are homeotically converted into carpels (e.g. (Modrusan et al., 1994)(Pautot et al., 2001)). In the latter case, one would expect to see multiple carpels growing within a single primary carpel. We never observed such a phenotype in *vip3* mutants, where instead the supernumerary organs all arose from the same stem or at least belonged to the same structure. It is therefore more likely that flower indeterminacy in *vip3* mutants is due to a delay in flower termination. To confirm that hypothesis, we generated longitudinal sections through carpels in both wild-type and *vip3* carpels, and stained the structures with toluidine blue. We observed that

supernumerary organs always developed within the primary carpels on a stem emerging from the bottom of the flower (Fig. 2, N=44 carpels). We never detected supernumerary organs emerging from ovules. The presence of such long stems within the carpel had not been reported in other indeterminate mutants such as *crc ult*, *crc sqn*, *crc rbl*, *pwd*, *clv1*, or *knu* (Prunet et al., 2008)(Yumul et al., 2013)(Clark et al., 1993)(Sun et al., 2009).

RNA-seq analysis of *vip3-1* mutant shoot apices reveals genomewide expression defects

Given the strength of the phenotype, we first checked whether specific pathways are affected in *vip3*. To do so, we performed a RNA-seq analysis of the *vip3-1* mutant, using shoot apices (Fig. S5A,B, see Material and methods). Note that this material only contained meristems and flowers up to stage 3 (i.e. not fully developed). The fold change for each gene is expressed in the log2 scale (meaning that a factor of e.g. 1 corresponds to a 2-fold change). This analysis revealed defect in *FLC* expression (down-regulation by a factor 4.6, Fig. S5C) as already reported (Oh et al., 2008). However, this large-scale analysis did not reveal clear-cut defects in specific flowering pathways, but rather global defects in the transcriptome, even if we cannot exclude any defects on specific pathways due to statistical and/or detailed annotations limitations. Genes from the same family (e.g. MADS) displayed either reduced (e.g. *AGL31, AGL77)* or enhanced (e.g. *AGL71*) mRNA accumulation in *vip3-1* (Fig. S5C). A few putative regulators of *WUS*, such as *ULT2,* exhibited a significant decrease of mRNA accumulation (by a factor 3.1), while *CLV3* mRNA accumulation was higher (by a factor 2.4) in *vip3-1* (Fig. S5C). Other putative regulators such as *PHB, ERL1, HAM3, PAN* also show higher mRNA accumulations but with lower rates (by factors 0.6, 0.8, 1 and 1.1, respectively, Fig. S5C). Similarly, we also found that hormone signaling pathways were affected, albeit without any clear-cut, specific trend. Yet, expression of genes involved in both auxin and cytokinin pathways seemed to be affected (Fig. S5D). Such data are consistent with previously reported phyllotactic defects in *vip3* (Fal et al., 2017), to recently published data on hormonal control of floral determinacy (Yamaguchi et al., 2018)(Zhang et al., 2018) as well as indeterminacy defects reported here. Note that the RNA-seq data obtained previously on *vip3* seedlings also reflected such genomewide alteration, without clear-cut targets (Oh et al., 2008). Altogether, these data are consistent with the hypothesis that the *vip3* mutant would not affect specific pathways, but rather increase transcriptional noise, as assessed in yeast (Ansel et al., 2008). Ideally, single cell RNA-seq analyses would provide quantitative data on transcriptional noise

in plants. These results thus call for gene-by-gene analysis of expression patterns of specific regulators of stem cell maintenance and flower termination.

Development of supernumerary organs result from the prolonged maintenance of stem cells in the center of the flower

As our phenotypic analysis suggests that the *vip3* indeterminacy phenotype is caused by a prolonged maintenance of stem cells in flowers, we focused our analysis on the integrator of stem cell maintenance and flower termination, *WUS*. Using *in situ* hybridization, we observed a bright and localized signal in the organizing center of wild-type SAM and young flowers until stage 5 or 6 (Fig. 3A, N_{WT}=34 flowers, (Mayer et al., 1998)). In *vip3*, we observed flowers with a similar pattern, but some others with more variable patterns. In particular, we could detect *WUS* expression at the center of flowers at a much later stage than in the wild type (Fig. 3A, Fig. S6B) which is consistent with the indeterminacy phenotype. *WUS* expression domain was also much broader than that of the wild type in certain *vip3* flowers (Fig. 3A, Fig. S6, $N_{vip3\text{-}1}$=30 flowers, $N_{vip3\text{-}2}$=45 flowers). To account for this variability in the spatial domain of *WUS* mRNA accumulation in *vip3*, we distinguished different types of patterns: whereas the wild type displayed a single robust pattern, the *vip3* mutant exhibited either a normal *WUS* expression domain (in 51 out of 73 meristems) or a larger and deeper *WUS* expression domain (in 22 out of 73 meristems, Fig. S6C). To further confirm these trends, we next analyzed the expression of *WUS* in a line expressing a fluorescently tagged under the control of *WUS* promoter (*pWUS::3xVENUS-N7* (Pfeiffer et al., 2016)). The fluorescent pattern was wider in both wild-type and mutant flowers, as compared to our *in situ* hybridization data. Wider *pWUS::GFP* expression domain in the wild type have already been reported (e.g. (Gordon et al., 2009)). Nevertheless, we clearly observed an even wider expression of *WUS* in *vip3* flowers, when compared to wild-type ones (Fig. 4A, N_{WT}=94 flowers, $N_{vip3\text{-}1}$=58 flowers). When quantifying the area of *WUS* expression, we found it to be up to twice larger in *vip3* than in the wild type (Fig. 4B). The coefficient of variation of *WUS* expression area was also significantly increased in *vip3* (Fig. S7A). The quantification of the average fluorescence intensity suggested a mild reduction of *WUS* promoter activity in *vip3*, although this might reflect a larger gradient domain (Fig. 4C). Based on both *in situ* hybridization data and fluorescent reporter lines, *WUS* expression domain appears variable and rather enlarged in *vip3*. As ectopic expression of *WUS* in flowers is also known to generate extra organ in the center of the flower (Lenhard et al., 2001), our data are consistent

with the macroscopic indeterminacy phenotype in *vip3*. Note that we could not detect a significant effect of the *vip3* mutation on the *CLV3* spatial expression domain by *in situ* hybridization. Yet, *CLV3* expression seemed to be maintained at later flower stages than in the wild type (in 6 out of 15 flower meristems beyond stage 6, Fig. S8, N_{WT}=10 meristems, 12 flowers, $N_{vip3\text{-}1}$= 9 meristems, 14 flowers, $N_{vip3\text{-}2}$=5 meristems, 5 flowers,). This is consistent with an overall delay in flower termination.

Mutation in *VIP3* results in a lower expression of AG in the center of the flower

Given that the *vip3* indeterminacy phenotype is strong and variable, and that it is associated with perturbed stem cell maintenance control, we analyzed the expression of the primary regulator of stem cell arrest in the flower, *AGAMOUS* (*AG*). Analysis of the *AG* mRNA pattern through *in situ* hybridization revealed the expected pattern in the wild type, with strong accumulations in floral whorls 3 and 4, prior to the emergence of stamens and carpels (Fig. 3B, N_{WT}=33 flowers). Similar patterns were also observed in certain *vip3* flowers, but *AG* mRNA accumulation appeared much reduced in the center of the whorl 4 in other flowers (Fig. 3B, $N_{vip3\text{-}1}$=35 flowers, $N_{vip3\text{-}2}$=12 flowers). To further confirm this result, we generated a fluorescently tagged version of AG under its own promoter (*pAG::AG-2xVenus*) and analyzed its expression profile. These data confirmed the results from the *in situ* hybridizations, while also showing a globally reduced level of AG in certain *vip3* flowers (Fig. 4A,C, N_{WT}=54 flowers, $N_{vip3\text{-}1}$=41 flowers). AG signal intensity was also more variable in *vip3* (Fig. S7B). The global area of AG expression was not significantly different in *vip3* and in the wild type, consistent with the observation that the contours were not strongly affected, and that only the center of flower exhibited defects in AG expression (Fig. 4B). Altogether, these results show that defects in Paf1c-dependent control of transcriptional noise lead to a delay in flower termination, notably through *AG* and *WUS* (Fig. 4D).

DISCUSSION

We have uncovered a strong floral indeterminacy phenotype in *vip3*. Flower development is usually considered to be highly robust in *Arabidopsis thaliana*. Nonetheless, chimeric flowers can be produced at rather low frequency (Hempel and Feldman, 1995). Such flowers result from primordia exhibiting both flowers and paraclades (lateral flowering shoot) features.

Here, *vip3* flowers develop normally (in term of identity) but, for a variable proportion, do not stop producing organs beyond stage 6 resulting in short and bumpy siliques up to completely open siliques containing a full inflorescence. Most indeterminacy phenotypes reported so far result in the production of extra floral organs, mostly carpels and stamens, rarely petals except in strong *ag* mutants that reiterate complete flowers (Bowman et al., 1989)(Prunet et al., 2009). Thus, in mutants with weaker phenotypes than that of *vip3*, floral meristem identity is never, or extremely rarely, lost. The only cases where a full new inflorescence was reported is in the *clv1-4* flowers where, in rare cases, a new inflorescence with developing flowers emerged from the gynoecium (Clark et al., 1993). Although this is obtained through gain of function, the *p35S::XAL2* line, in which the MADS box transcription factor XAL2/AGL14 is overexpressed, also displays major indeterminacy defects, resembling that of *vip3* mutants (Pérez-Ruiz et al., 2015). Our results in *vip3* mutants suggest that full reversion may be reachable through a more global perturbation of transcription. This calls for a more systemic investigation of the molecular players behind floral indeterminacy. In fact, these results also question the limits of the reductionist approach: genetic screens for floral indeterminacy did not uncover the *vip3* mutant so far, either because growth conditions were not appropriate, or because variable phenotypes are less likely to be identified and selected.

Early stages of growth in short day conditions appeared essential to trigger the indeterminacy phenotype in *vip3*. This might be consistent with the reported role of the Paf1 complex in the regulation of flowering time and *FLC* expression (Zhang et al., 2003). This also reveals that a rather late phenotype (carpel differentiation) depends on very early cues during development. Our findings thus suggest that floral indeterminacy is much more plastic than anticipated, integrating the larger plant status, early on in development. The indeterminacy defects are not detected in long day conditions, but are observed in short day or continuous light conditions. Given that the latter growth conditions enhance meristem size (Hamant et al., 2014), it is possible that a threshold in meristem size is required for the indeterminacy phenotype to exist. In this respect, cytokinins are likely to play a strong integrator role, given their known impact on the regulation of *WUS* expression and meristem size (Pfeiffer et al., 2016)(Landrein et al., 2018). Beyond cytokinins, the larger hormonal network is likely to be involved. For instance, in our RNA-seq analysis, we also find that YUC4, a target of AG and CRC (Yamaguchi et al., 2018), is down-regulated in *vip3-1*. It remains to be shown whether

such conclusions apply to other species; data in impatiens may suggest that it is the case (Pouteau et al., 1997).

As *AG* is deregulated in *vip3* mutants, our study also introduces Paf1c as a new player in the flower termination pathway. The use of lines expressing the antisense *AG* RNA reported a range of phenotype spanning from a weak indeterminacy phenotype (normal flower with few extra organs developing inside the primary carpels) to the canonical *ag* phenotype ([sepals-petals-petals]n), each category corresponding to a lower level of endogenous *AG* expression (Mizukami and Ma, 1995). In *vip3*, we observed weaker AG expression in the floral domain that corresponds to the 4th whorl subdomain that develop carpel margins and placenta. The reduced AG level in *vip3* may be consistent with the reported increase in H3K27me3 over the *AG* region in the mutant (see Figure S4 in (Oh et al., 2008)). Our study thus opens the possibility that part of the plasticity in carpel development relies on Paf1c-dependent *AG* expression.

Lastly, our results echo the rising role of incomplete penetrance in developmental plasticity. Incomplete penetrance is intrinsically caused by random fluctuations in gene expression (Raj and van Oudenaarden, 2008). Such variability contribute to cell fate specification in multicellular organisms (Chang et al., 2008)(Hume, 2000)(Wernet et al., 2006). The existence of such variability may lead to incoherencies in gene networks; yet it would also provide a way for the network to become less sensitive to environmental fluctuations. In other words, cells would still retain the ability to acquire alternative fates, despite the channeling effect of environmental cues (Hart et al., 2014). Interestingly, we find that the *vip3* indeterminacy phenotype occurs when in the wild type, *WUS* expression slowly decreases in flowers. Gene expression fading (in and out) and low levels of gene expression might represent weak points in gene networks, as variability in gene expression (area, intensity, and duration) in such instances may have more pronounced effects. Conversely, the gene regulatory network often promotes clear-cut expression patterns (both in space and time), and this may limit the presence of such weak points. It may appear surprising that a developmental switch as important as the decision to stop or maintain stem cells in a flower would rely on such a robust Boolean control, yet our results in the *vip3* mutant suggests that increased transcriptional noise is sufficient to induce indeterminacy. This calls for an analysis of the adaptive benefits of such a weak control. One may speculate that the number of fruits

and seeds could be increased *via* this unusual prolongation of floral stem cell competence, as observed in other species (see e.g. (Tooke et al., 2005)).

MATERIAL AND METHODS

Plant lines

All procedures were performed on plants from the Col-0 ecotype. The *pWUS::3xVENUS-N7* reporter lines (Pfeiffer et al., 2016) and T-DNA insertion lines *vip3-1* (salk139885) and *vip3-2* (salk083364) were used for this study (genotyping primers are listed in Table S1). To generate the *pAG::AG-2xVenus* line, we used a fragment of genomic *AG* from Col-0, containing 2655 bp of upstream sequence, the 1061 bp long 5'UTR (which includes intron 1) and 4241 bp from start to stop (which includes the 2999 bp long second intron), amplified with the pPD381 and pPD413 primers (see Table S1) and transferred with XmaI digestion in BJ36 containing 2xVenus fluorescent reporter. BJ36 with 2xVenus was obtained from pCS2-Venus with pPD441 and pPD442 primers (see Table S1) adding 5xAla at the beginning of Venus and transferred twice in BJ36 through BamHI and XmaI digestion. The *pAG::AG-2xVenus* obtain fragment was transferred in *pART* (a kanamycin resistant vector) with XmaI digestion and then transformed in Col-0 plants using *Agrobacterium tumefaciens*.

Growth conditions

In "short day" conditions, plants were grown under a 8hr (20°C) / 16hr (15°C) light/dark period. In "long day" conditions, plants were grown under a 16hr (21°C) / 8hr (19°C) light/dark period. In continuous light conditions, plants were grown under continuous light at 16°C or 21°C. In "short day then long day or continuous light conditions", plants were first grown for 3 weeks in short day conditions and then transferred to long day or continuous light conditions.

RNA-seq analysis of *vip3* shoot apices

vip3-1 and Col-0 shoot apices (from plants grown in short day 21°C then continuous light 16°C conditions) were dissected, by removing flower older than stage 4. Samples were collected into liquid nitrogen-cooled eppendorf tubes directly after dissection, each tube containing between 30 and 35 apices, 6 samples for each genotype. RNA extraction was performed using the PicoPure RNA Isolation kit Arcturus (ThermoFisher, KIT0204) with an

on column DNAase treatment (Qiagen, catalog#79254). After elution, 2 samples were combined together, obtaining the final technical triplicates for each genotype. RNA concentrations in the samples were measured by Bioanalyser (Plant RNA Nano Assay, Agilent Technologies, Chip priming station number 5065- 4401, 16-pin bayonet electrode cartridge order number 5065- 4413) and sent for sequencing. Total RNA libraries preparation, Illumina sequencing and initial data analysis were performed by Fasteris: HiSeq instrument, Basecalling pipeline, HiSeq Control Software HD 3.4.0.38, analysed with Expression_mRNA_tuxedo. Adapter trimming – with Trimmomatic: A flexible read trimming tool for Illumina NGS data (Bolger, A. M., Lohse, M., & Usadel, B., 2014. Trimmomatic: A flexible trimmer for Illumina Sequence Data. Bioinformatics, btu170). Mapping - with BOWTIE 2.0.5 (Langmead et al., 2009), TOPHAT 2.0.6 (http://tophat.cbcb.umd.edu/), SAMTOOLS 1.2 (http://www.htslib.org/). Reference genome - *Arabidopsis thaliana* Ensembly TAIR10, from iGenome. Expression estimation, normalization and comparison – CUFFLINKS v2.1.1 (http://cufflinks.cbcb.umd.edu/).

Histological sections and *in situ* hybridization

The *in situ* hybridization on paraplast–embedded tissues was performed as described in (Vernoux et al., 2011). Shoot apices were sectioned into 8 µm thick slices. The probes for the coding regions of *WUS* and *AG* were amplified with specific primers (listed in the Table S1), where the T7 promoter sequence was added to the reverse primer. PCR products were further purified with the QIAquick PCR Purification Kit (QIAGEN Cat No./ID: 28106). *In vitro* transcription and DIG labeling of the probes were performed with the T7 RNA polymerase (Promega, #P2077) and DIG RNA Labeling Mix (Roche #11277073910). For histological sections, late flowers (stage15-16) were harvested and paraplast–embedded following the same protocol. After sectioning, paraffin removal and rehydration, the samples were stained with 0.1% toluidine blue solution. Images were acquired using the Zeiss Imager.M2 microscope (20x and 40x objectives) and the Axiocam 503. Results were obtained in triplicates (3 independent rounds of *in situ* hybridizations, from independently grown plant populations).

Confocal laser scanning microscopy and image analysis

Dissected meristems and plants grown *in vitro* were imaged with a water dipping lens (x25, NA = 0.8) using a SP8 confocal microscope (Leica, Germany) to generate stack of optical

sections with an interval of 0.2 µm between slices. The membranes were stained with FM4-64. Image analysis was performed using the Fiji software (http://fiji.sc/wiki/index.php/Fiji). The fluorescence intensity and size of the fluorescent area were extracted from the maximum projections of the image stacks of each individual flowers using the ROI tool. For smaller flowers, ca. 280 slices were imaged, representing a 56µm-thick stack; for older flowers, ca. 430 slices were imaged representing a 87µm-thick stack. Average diameter of the flowers was calculated by tracing 4 lines between the edges of a flower, crossing in the center with a 45° angle between each 2 of them. The extracted ROI values were further analyzed using Microsoft Excel. Statistical analysis was performed using either Microsoft Excel or R softwares. The two-tailed Student test was performed to compare means of independent biological replicates. Results were obtained in triplicates (3 independent rounds of imaging sessions, from independently grown plant populations).

Acknowledgements

We thank Toshiro Ito for constructive discussions around this project and our colleagues for critical reading of this manuscript. We also thank Platim for help with imaging. We acknowledge Jan Lohmann for providing the *pWUS::3xVENUS-N7* reporter line. We also thank the anonymous reviewers for their constructive comments.

Competing interests

The authors declare no competing or financial interests.

Author contributions

K.F., C.T. and O.H. conceived and designed the experiments. K.F., M.C. and M.L. performed the experiments. S.C. and P.D. provided important material for this study. K.F., M.C., O.H. and C.T. wrote the manuscript.

Funding

This work was supported by the European Research Council Grants 615739 “MechanoDevo”, the “Fondation Schlumberger pour l’Education et la Recherche”, and ANRT CIFRE contract n°2017/0975.

References

Alemu, E. Y., Carl, J. W., Corrada Bravo, H. and Hannenhalli, S. (2014). Determinants of expression variability. *Nucleic Acids Res.* **42**, 3503–3514.

Ansel, J., Bottin, H., Rodriguez-Beltran, C., Damon, C., Nagarajan, M., Fehrmann, S., François, J. and Yvert, G. (2008). Cell-to-Cell Stochastic Variation in Gene Expression Is a Complex Genetic Trait. *PLoS Genetics* **4**, e1000049.

Antosz, W., Pfab, A., Ehrnsberger, H. F., Holzinger, P., Köllen, K., Mortensen, S. A., Bruckmann, A., Schubert, T., Längst, G., Griesenbeck, J., et al. (2017). The Composition of the Arabidopsis RNA Polymerase II Transcript Elongation Complex Reveals the Interplay between Elongation and mRNA Processing Factors. *Plant Cell* **29**, 854–870.

Besnard, F., Vernoux, T. and Hamant, O. (2011). Organogenesis from stem cells in planta: multiple feedback loops integrating molecular and mechanical signals. *Cell Mol Life Sci* **68**, 2885–2906.

Bollier, N., Sicard, A., Leblond, J., Latrasse, D., Gonzalez, N., Gévaudant, F., Benhamed, M., Raynaud, C., Lenhard, M., Chevalier, C., et al. (2018). At-MINI ZINC FINGER2 and Sl-INHIBITOR OF MERISTEM ACTIVITY, a Conserved Missing Link in the Regulation of Floral Meristem Termination in Arabidopsis and Tomato. *The Plant Cell* **30**, 83–100.

Bowman, J. L., Smyth, D. R. and Meyerowitz, E. M. (1989). Genes directing flower development in Arabidopsis. *Plant Cell* **1**, 37–52.

Brand, U. (2000). Dependence of Stem Cell Fate in Arabidopsis on a Feedback Loop Regulated by CLV3 Activity. *Science* **289**, 617–619.

Carles, C. C. (2005). ULTRAPETALA1 encodes a SAND domain putative transcriptional regulator that controls shoot and floral meristem activity in Arabidopsis. *Development* **132**, 897–911.

Chang, H. H., Hemberg, M., Barahona, M., Ingber, D. E. and Huang, S. (2008). Transcriptome-wide noise controls lineage choice in mammalian progenitor cells. *Nature* **453**, 544–547.

Chen, F. X., Xie, P., Collings, C. K., Cao, K., Aoi, Y., Marshall, S. A., Rendleman, E. J., Ugarenko, M., Ozark, P. A., Zhang, A., et al. (2017). PAF1 regulation of promoter-proximal pause release via enhancer activation. *Science* **357**, 1294–1298.

Clark, S. E., Running, M. P. and Meyerowitz, E. M. (1993). CLAVATA1, a regulator of meristem and flower development in Arabidopsis. *Development* **119**, 397–418.

Claßen-Bockhoff, R. and Bull-Hereñu, K. (2013). Towards an ontogenetic understanding of inflorescence diversity. *Annals of Botany* **112**, 1523–1542.

Das, P., Ito, T., Wellmer, F., Vernoux, T., Dedieu, A., Traas, J. and Meyerowitz, E. M. (2009). Floral stem cell termination involves the direct regulation of AGAMOUS by PERIANTHIA. *Development* **136**, 1605–1611.

Daum, G., Medzihradszky, A., Suzaki, T. and Lohmann, J. U. (2014). A mechanistic framework for noncell autonomous stem cell induction in Arabidopsis. *Proc. Natl. Acad. Sci. U.S.A.* **111**, 14619–14624.

Dorcey, E., Rodriguez-Villalon, A., Salinas, P., Santuari, L., Pradervand, S., Harshman, K. and Hardtke, C. S. (2012). Context-dependent dual role of SKI8 homologs in mRNA synthesis and turnover. *PLoS Genet.* **8**, e1002652.

Fal, K., Liu, M., Duisembekova, A., Refahi, Y., Haswell, E. S. and Hamant, O. (2017). Phyllotactic regularity requires the Paf1 complex in Arabidopsis. *Development* **144**, 4428–4436.

Fletcher, J. C. (2001). The ULTRAPETALA gene controls shoot and floral meristem size in Arabidopsis. *Development* **128**, 1323–1333.

Gordon, S. P., Chickarmane, V. S., Ohno, C. and Meyerowitz, E. M. (2009). Multiple feedback loops through cytokinin signaling control stem cell number within the Arabidopsis shoot meristem. *Proc. Natl. Acad. Sci. U.S.A.* **106**, 16529–16534.

Green, K. A., Prigge, M. J., Katzman, R. B. and Clark, S. E. (2005). *CORONA* , a Member of the Class III Homeodomain Leucine Zipper Gene Family in Arabidopsis, Regulates Stem Cell Specification and Organogenesis. *The Plant Cell* **17**, 691–704.

Gruel, J., Landrein, B., Tarr, P., Schuster, C., Refahi, Y., Sampathkumar, A., Hamant, O., Meyerowitz, E. M. and Jönsson, H. (2016). An epidermis-driven mechanism positions and scales stem cell niches in plants. *Sci. Adv.* 2 : e1500989.

Guo, L., Cao, X., Liu, Y., Li, J., Li, Y., Li, D., Zhang, K., Gao, C., Dong, A. and Liu, X. (2018). A chromatin loop represses *WUSCHEL* expression in Arabidopsis. *The Plant Journal* **94**, 1083–1097.

Hamant, O., Das, P. and Burian, A. (2014). Time-lapse imaging of developing meristems using confocal laser scanning microscope. *Methods Mol Biol* **1080**, 111–119.

Hart, Y., Reich-Zeliger, S., Antebi, Y. E., Zaretsky, I., Mayo, A. E., Alon, U. and Friedman, N. (2014). Paradoxical Signaling by a Secreted Molecule Leads to Homeostasis of Cell Levels. *Cell* **158**, 1022–1032.

He, Y., Doyle, M. R. and Amasino, R. M. (2004). PAF1-complex-mediated histone methylation of FLOWERING LOCUS C chromatin is required for the vernalization-responsive, winter-annual habit in Arabidopsis. *Genes Dev.* **18**, 2774–2784.

Hempel, F. D. and Feldman, L. J. (1995). Specification of chimeric flowering shoots in wild-type Arabidopsis. *The Plant Journal* **8**, 725–731.

Huang, Z., Shi, T., Zheng, B., Yumul, R. E., Liu, X., You, C., Gao, Z., Xiao, L. and Chen, X.

(2017). *APETALA2* antagonizes the transcriptional activity of *AGAMOUS* in regulating floral stem cells in *Arabidopsis thaliana*. *New Phytologist* **215**, 1197–1209.

Hume, D. A. (2000). Probability in transcriptional regulation and its implications for leukocyte differentiation and inducible gene expression. *Blood* **96**, 2323–2328.

Irish, V. F. and Sussex, I. M. (1990). Function of the apetala-1 gene during Arabidopsis floral development. *Plant Cell* **2**, 741–753.

Kaya, H., Shibahara, K., Taoka, K., Iwabuchi, M., Stillman, B. and Araki, T. (2001). FASCIATA Genes for Chromatin Assembly Factor-1 in Arabidopsis Maintain the Cellular Organization of Apical Meristems. *Cell* **104**, 131–142.

Kinoshita, A., Betsuyaku, S., Osakabe, Y., Mizuno, S., Nagawa, S., Stahl, Y., Simon, R., Yamaguchi-Shinozaki, K., Fukuda, H. and Sawa, S. (2010). RPK2 is an essential receptor-like kinase that transmits the CLV3 signal in Arabidopsis. *Development* **137**, 3911–3920.

Kwon, C. S. (2005). WUSCHEL is a primary target for transcriptional regulation by SPLAYED in dynamic control of stem cell fate in Arabidopsis. *Genes & Development* **19**, 992–1003.

Landrein, B., Formosa-Jordan, P., Malivert, A., Schuster, C., Melnyk, C. W., Yang, W., Turnbull, C., Meyerowitz, E. M., Locke, J. C. W. and Jönsson, H. (2018). Nitrate modulates stem cell dynamics in Arabidopsis shoot meristems through cytokinins. *Proc. Natl. Acad. Sci. U.S.A.* **115**, 1382–1387.

Langmead, B., Trapnell, C., Pop, M. and Salzberg, S. L. (2009). Ultrafast and memory-efficient alignment of short DNA sequences to the human genome. *Genome Biology* **10**, R25.

Leibfried, A., To, J. P. C., Busch, W., Stehling, S., Kehle, A., Demar, M., Kieber, J. J. and Lohmann, J. U. (2005). WUSCHEL controls meristem function by direct regulation of cytokinin-inducible response regulators. *Nature* **438**, 1172–1175.

Lenhard, M. and Laux, T. (2003). Stem cell homeostasis in the Arabidopsis shoot meristem is regulated by intercellular movement of CLAVATA3 and its sequestration by CLAVATA1. *Development* **130**, 3163–3173.

Lenhard, M., Bohnert, A., Jürgens, G. and Laux, T. (2001). Termination of stem cell maintenance in Arabidopsis floral meristems by interactions between WUSCHEL and AGAMOUS. *Cell* **105**, 805–814.

Liu, X., Kim, Y. J., Muller, R., Yumul, R. E., Liu, C., Pan, Y., Cao, X., Goodrich, J. and Chen, X. (2011). AGAMOUS Terminates Floral Stem Cell Maintenance in Arabidopsis by Directly Repressing WUSCHEL through Recruitment of Polycomb Group Proteins. *The Plant Cell* **23**, 3654–3670.

Liu, X., Dinh, T. T., Li, D., Shi, B., Li, Y., Cao, X., Guo, L., Pan, Y., Jiao, Y. and Chen, X. (2014). *AUXIN RESPONSE FACTOR 3* integrates the functions of *AGAMOUS* and *APETALA2* in floral meristem determinacy. *The Plant Journal* **80**, 629–641.

Lohmann, J. U., Hong, R. L., Hobe, M., Busch, M. A., Parcy, F., Simon, R. and Weigel, D. (2001). A molecular link between stem cell regulation and floral patterning in Arabidopsis. *Cell* **105**, 793–803.

Maier, A. T., Stehling-Sun, S., Wollmann, H., Demar, M., Hong, R. L., Haubeiss, S., Weigel, D. and Lohmann, J. U. (2009). Dual roles of the bZIP transcription factor PERIANTHIA in the control of floral architecture and homeotic gene expression. *Development* **136**, 1613–1620.

Mandel, A. M., Gustafson-Brown, C., Savidge, B. and Yanofsky, M. F. (1992). Molecular characterization of the Arabidopsis floral homeotic gene APETALA1. *Nature* **360**, 273–277.

Mandel, T., Moreau, F., Kutsher, Y., Fletcher, J. C., Carles, C. C. and Williams, L. E. (2014). The ERECTA receptor kinase regulates Arabidopsis shoot apical meristem size, phyllotaxy and floral meristem identity. *Development* **141**, 830–841.

Mandel, T., Candela, H., Landau, U., Asis, L., Zelinger, E., Carles, C. C. and Williams, L. E. (2016). Differential regulation of meristem size, morphology and organization by the ERECTA, CLAVATA and class III HD-ZIP pathways. *Development* **143**, 1612–1622.

Mantsoki, A., Devailly, G. and Joshi, A. (2016). Gene expression variability in mammalian embryonic stem cells using single cell RNA-seq data. *Computational Biology and Chemistry* **63**, 52–61.

Mason, E. A., Mar, J. C., Laslett, A. L., Pera, M. F., Quackenbush, J., Wolvetang, E. and Wells, C. A. (2014). Gene Expression Variability as a Unifying Element of the Pluripotency Network. *Stem Cell Reports* **3**, 365–377.

Mayer, K. F., Schoof, H., Haecker, A., Lenhard, M., Jürgens, G. and Laux, T. (1998). Role of WUSCHEL in regulating stem cell fate in the Arabidopsis shoot meristem. *Cell* **95**, 805–815.

Meyer, H. M., Teles, J., Formosa-Jordan, P., Refahi, Y., San-Bento, R., Ingram, G., Jönsson, H., Locke, J. C. W. and Roeder, A. H. K. (2017). Fluctuations of the transcription factor ATML1 generate the pattern of giant cells in the Arabidopsis sepal. *Elife* **6**,.

Mizukami, Y. and Ma, H. (1995). Separation of AG function in floral meristem determinacy from that in reproductive organ identity by expressing antisense AG RNA. *Plant Mol. Biol.* **28**, 767–784.

Modrusan, Z., Reiser, L., Feldmann, K. A., Fischer, R. L. and Haughn, G. W. (1994). Homeotic Transformation of Ovules into Carpel-like Structures in Arabidopsis. *Plant Cell* **6**, 333–349.

Momiji, H. and Monk, N. A. M. (2009). Oscillatory Notch-pathway activity in a delay model of neuronal differentiation. *Phys Rev E Stat Nonlin Soft Matter Phys* **80**, 021930.

Monfared, M. M., Carles, C. C., Rossignol, P., Pires, H. R. and Fletcher, J. C. (2013). The ULT1 and ULT2 trxG genes play overlapping roles in Arabidopsis development and gene regulation. *Mol Plant* **6**, 1564–1579.

Muller, R., Bleckmann, A. and Simon, R. (2008). The Receptor Kinase CORYNE of Arabidopsis Transmits the Stem Cell-Limiting Signal CLAVATA3 Independently of CLAVATA1. *THE PLANT CELL ONLINE* **20**, 934–946.

Oh, S., Zhang, H., Ludwig, P. and van Nocker, S. (2004). A mechanism related to the yeast transcriptional regulator Paf1c is required for expression of the Arabidopsis FLC/MAF MADS box gene family. *Plant Cell* **16**, 2940–2953.

Oh, S., Park, S. and van Nocker, S. (2008). Genic and global functions for Paf1C in chromatin modification and gene expression in Arabidopsis. *PLoS Genet.* **4**, e1000077.

Padovan-Merhar, O. and Raj, A. (2013). Using variability in gene expression as a tool for studying gene regulation: Characterizing gene regulation using expression variability. *Wiley Interdisciplinary Reviews: Systems Biology and Medicine* **5**, 751–759.

Pautot, V., Dockx, J., Hamant, O., Kronenberger, J., Grandjean, O., Jublot, D. and Traas, J. (2001). KNAT2: evidence for a link between knotted-like genes and carpel development. *Plant Cell* **13**, 1719–1734.

Pérez-Ruiz, R. V., García-Ponce, B., Marsch-Martínez, N., Ugartechea-Chirino, Y., Villajuana-Bonequi, M., de Folter, S., Azpeitia, E., Dávila-Velderrain, J., Cruz-Sánchez, D., Garay-Arroyo, A., et al. (2015). XAANTAL2 (AGL14) Is an Important Component of the Complex Gene Regulatory Network that Underlies Arabidopsis Shoot Apical Meristem Transitions. *Mol Plant* **8**, 796–813.

Pfeiffer, A., Janocha, D., Dong, Y., Medzihradszky, A., Schöne, S., Daum, G., Suzaki, T., Forner, J., Langenecker, T., Rempel, E., et al. (2016). Integration of light and metabolic signals for stem cell activation at the shoot apical meristem. *eLife* **5**,.

Pfeiffer, A., Wenzl, C. and Lohmann, J. U. (2017). Beyond flexibility: controlling stem cells in an ever changing environment. *Current Opinion in Plant Biology* **35**, 117–123.

Pouteau, S., Nicholls, D., Tooke, F., Coen, E. and Battey, N. (1997). The induction and maintenance of flowering in Impatiens. *Development* **124**, 3343–3351.

Prigge, M. J., Otsuga, D., Alonso, J. M., Ecker, J. R., Drews, G. N. and Clark, S. E. (2005). Class III Homeodomain-Leucine Zipper Gene Family Members Have Overlapping, Antagonistic, and Distinct Roles in Arabidopsis Development. *The Plant Cell* **17**, 61–76.

Prunet, N., Morel, P., Thierry, A.-M., Eshed, Y., Bowman, J. L., Negrutiu, I. and Trehin, C. (2008). REBELOTE, SQUINT, and ULTRAPETALA1 Function Redundantly in the Temporal Regulation of Floral Meristem Termination in Arabidopsis thaliana. *THE PLANT CELL ONLINE* **20**, 901–919.

Prunet, N., Morel, P., Negrutiu, I. and Trehin, C. (2009). Time to stop: flower meristem termination. *Plant Physiol.* **150**, 1764–1772.

Raj, A. and van Oudenaarden, A. (2008). Nature, nurture, or chance: stochastic gene expression and its consequences. *Cell* **135**, 216–226.

Raj, A., Rifkin, S. A., Andersen, E. and van Oudenaarden, A. (2010). Variability in gene expression underlies incomplete penetrance. *Nature* **463**, 913–918.

Richard, M. and Yvert, G. (2014). How does evolution tune biological noise? *Frontiers in Genetics* **5**,.

Rojo, E. (2002). CLV3 Is Localized to the Extracellular Space, Where It Activates the Arabidopsis CLAVATA Stem Cell Signaling Pathway. *THE PLANT CELL ONLINE* **14**, 969–977.

Schoof, H., Lenhard, M., Haecker, A., Mayer, K. F., Jürgens, G. and Laux, T. (2000). The stem cell population of Arabidopsis shoot meristems in maintained by a regulatory loop between the CLAVATA and WUSCHEL genes. *Cell* **100**, 635–644.

Smyth, D. R., Bowman, J. L. and Meyerowitz, E. M. (1990). Early flower development in Arabidopsis. *Plant Cell* **2**, 755–767.

Somssich, M., Je, B. I., Simon, R. and Jackson, D. (2016). CLAVATA-WUSCHEL signaling in the shoot meristem. *Development* **143**, 3238–3248.

Sprinzak, D., Lakhanpal, A., LeBon, L., Santat, L. A., Fontes, M. E., Anderson, G. A., Garcia-Ojalvo, J. and Elowitz, M. B. (2010). Cis-interactions between Notch and Delta generate mutually exclusive signalling states. *Nature* **465**, 86–90.

Sun, B., Xu, Y., Ng, K.-H. and Ito, T. (2009). A timing mechanism for stem cell maintenance and differentiation in the Arabidopsis floral meristem. *Genes & Development* **23**, 1791–1804.

Sun, B., Looi, L.-S., Guo, S., He, Z., Gan, E.-S., Huang, J., Xu, Y., Wee, W.-Y. and Ito, T. (2014). Timing Mechanism Dependent on Cell Division Is Invoked by Polycomb Eviction in Plant Stem Cells. *Science* **343**, 1248559–1248559.

Sun, B., Zhou, Y., Cai, J., Shang, E., Yamaguchi, N., Xiao, J., Looi, L.-S., Wee, W.-Y., Gao, X., Wagner, D., et al. (2019). Integration of Transcriptional Repression and Polycomb-Mediated Silencing of *WUSCHEL* in Floral Meristems. *The Plant Cell* **31**, 1488–1505.

Takagi, N. and Ueguchi, C. (2012). Enhancement of meristem formation by bouquet-1, a mis-sense allele of the vernalization independence 3 gene encoding a WD40 repeat protein in Arabidopsis thaliana. *Genes Cells* **17**, 982–993.

Tooke, F., Ordidge, M., Chiurugwi, T. and Battey, N. (2005). Mechanisms and function of flower and inflorescence reversion. *Journal of Experimental Botany* **56**, 2587–2599.

Tsugawa, S., Hervieux, N., Kierzkowski, D., Routier-Kierzkowska, A.-L., Sapala, A., Hamant, O., Smith, R. S., Roeder, A. H. K., Boudaoud, A. and Li, C.-B. (2017). Clones of cells switch from reduction to enhancement of size variability in Arabidopsis sepals. *Development* **144**, 4398–4405.

Vernoux, T., Brunoud, G., Farcot, E., Morin, V., Van den Daele, H., Legrand, J., Oliva, M., Das, P., Larrieu, A., Wells, D., et al. (2011). The auxin signalling network translates dynamic input into robust patterning at the shoot apex. *Mol. Syst. Biol.* **7**, 508.

Wang, J., Liu, D., Guo, X., Yang, W., Wang, X., Zhan, K. and Zhang, A. (2011). Variability of Gene Expression After Polyhaploidization in Wheat (*Triticum aestivum* L.). *G3: Genes|Genomes|Genetics* **1**, 27–33.

Waters, A. J., Makarevitch, I., Noshay, J., Burghardt, L. T., Hirsch, C. N., Hirsch, C. D. and Springer, N. M. (2017). Natural variation for gene expression responses to abiotic stress in maize. *The Plant Journal* **89**, 706–717.

Wernet, M. F., Mazzoni, E. O., Celik, A., Duncan, D. M., Duncan, I. and Desplan, C. (2006). Stochastic spineless expression creates the retinal mosaic for colour vision. *Nature* **440**, 174–180.

Williams, L. (2005). Regulation of Arabidopsis shoot apical meristem and lateral organ formation by microRNA miR166g and its AtHD-ZIP target genes. *Development* **132**, 3657–3668.

Xu, Q., Zhu, C., Fan, Y., Song, Z., Xing, S., Liu, W., Yan, J. and Sang, T. (2016). Population transcriptomics uncovers the regulation of gene expression variation in adaptation to changing environment. *Scientific Reports* **6**,.

Yadav, R. K., Perales, M., Gruel, J., Girke, T., Jönsson, H. and Reddy, G. V. (2011). WUSCHEL protein movement mediates stem cell homeostasis in the Arabidopsis shoot apex. *Genes Dev.* **25**, 2025–2030.

Yamaguchi, N., Huang, J., Tatsumi, Y., Abe, M., Sugano, S. S., Kojima, M., Takebayashi, Y., Kiba, T., Yokoyama, R., Nishitani, K., et al. (2018). Chromatin-mediated feed-forward auxin biosynthesis in floral meristem determinacy. *Nature Communications* **9**,.

Yanofsky, M. F., Ma, H., Bowman, J. L., Drews, G. N., Feldmann, K. A. and Meyerowitz, E. M. (1990). The protein encoded by the Arabidopsis homeotic gene agamous resembles transcription factors. *Nature* **346**, 35–39.

Yumul, R. E., Kim, Y. J., Liu, X., Wang, R., Ding, J., Xiao, L. and Chen, X. (2013). POWERDRESS and Diversified Expression of the MIR172 Gene Family Bolster the Floral Stem Cell Network. *PLoS Genetics* **9**, e1003218.

Zhang, H., Ransom, C., Ludwig, P. and van Nocker, S. (2003). Genetic analysis of early flowering mutants in Arabidopsis defines a class of pleiotropic developmental regulator required for expression of the flowering-time switch flowering locus C. *Genetics* **164**, 347–358.

Zhang, K., Wang, R., Zi, H., Li, Y., Cao, X., Li, D., Guo, L., Tong, J., Pan, Y., Jiao, Y., et al. (2018). AUXIN RESPONSE FACTOR3 Regulates Floral Meristem Determinacy by Repressing Cytokinin Biosynthesis and Signaling. *The Plant Cell* **30**, 324–346.

Zhao, L., Kim, Y., Dinh, T. T. and Chen, X. (2007). miR172 regulates stem cell fate and defines the inner boundary of APETALA3 and PISTILLATA expression domain in Arabidopsis floral meristems. *Plant J.* **51**, 840–849.

Zhou, Y., Yan, A., Han, H., Li, T., Geng, Y., Liu, X. and Meyerowitz, E. M. (2018). HAIRY MERISTEM with WUSCHEL confines CLAVATA3 expression to the outer apical meristem layers. *Science* **361**, 502–506.

Figures

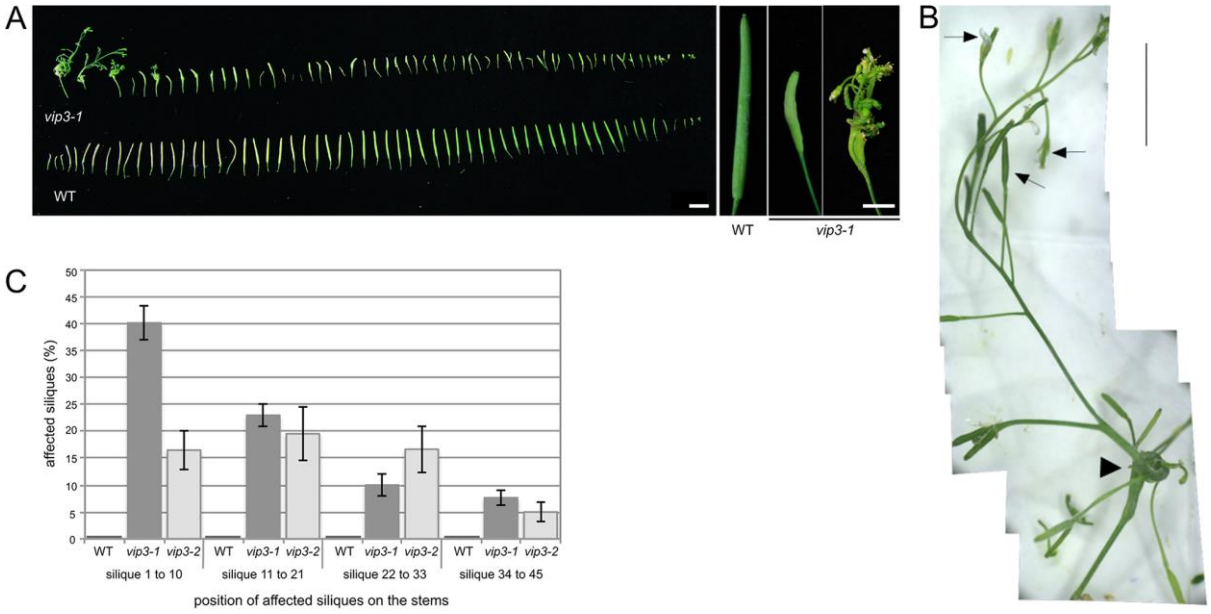

Fig. 1. *vip3* mutants can exhibit a severe flower indeterminacy phenotype.

(A) Representative phenotype of wild-type and *vip3* siliques, from plants grown in short day 21°C then continuous light 16°C conditions (N>30 plants), harvested in a sequence of initiation from the stems of (left panel). Scale bar: 1 cm. Right panel: representative siliques of the wild type and *vip3* displaying different degrees of phenotypic defects. Scale bar: 5 mm. (B) Representative image of the most severe phenotype in *vip3-1* flowers. Arrowhead points at the primary silique; arrows point at secondary carpels. Scale bar: 1 cm. (C) Distribution (%) of affected siliques on the stems of the wild type (N=13), *vip3-1* (N=60) and *vip3-2* (N=20) grown in short day 21°C followed by continuous light 16°C condition (on average, 20% of *vip3-1* and 14% of *vip3-2* siliques displayed visible indeterminacy defects in these conditions).

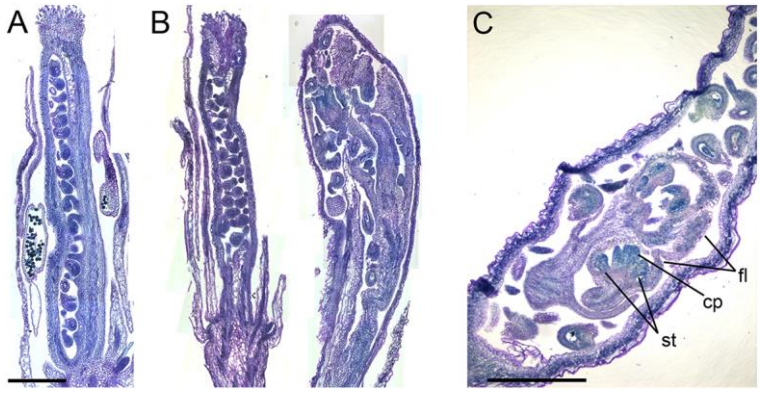

Fig. 2. Inflorescence stem and floral organs can be detected in *vip3* siliques.

(A-C) Sections in young siliques, stained with toluidine blue. WT (A) and representative *vip3* (B) siliques that illustrate the spectrum of *vip3* phenotypes. (C) Section of *vip3* silique that demonstrates the presence of floral structures (fl – flower, cp – carpels, st – stamens) inside the silique. Scale bars : 500 μm.

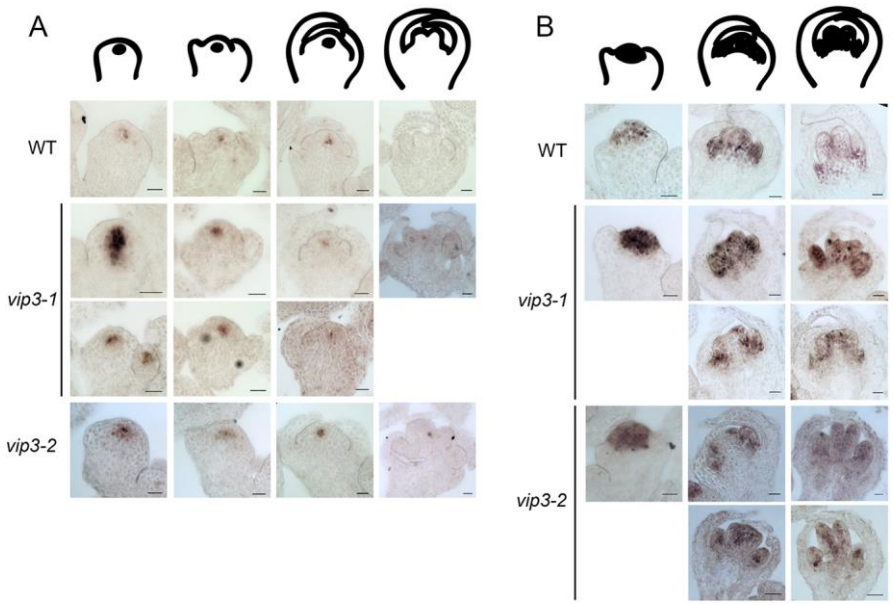

Fig. 3. Expression patterns of *WUS* and *AG* in *vip3* flowers.

Representative *in situ* hybridization of *WUS* (A, N_{WT}=34 flowers, $N_{vip3\text{-}1}$=30 flowers, $N_{vip3\text{-}2}$=45 flowers) and *AG* (B, N_{WT}=33 flowers, $N_{vip3\text{-}1}$=35 flowers, $N_{vip3\text{-}2}$=12 flowers) transcripts in wild-type and *vip3 (vip3-1* and *vip3-2)* flowers at four or three different developmental stages (as represented by schematic drawings). Plants for hybridization were grown in short day then continuous light 16°C conditions (as in Fig. 1). Scale bars : 20 µm.

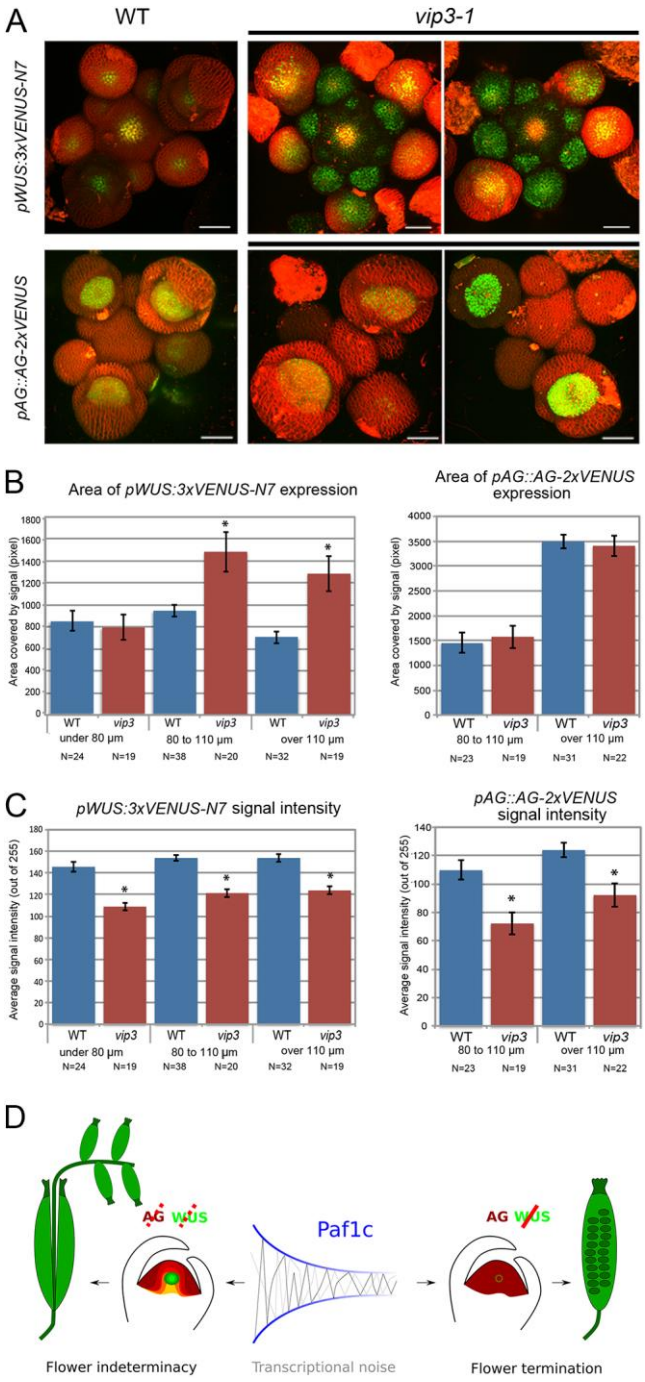

Fig. 4. Expression of *WUS* and *AG* reporter lines in *vip3* flowers.

(A) Representative wild-type and *vip3-1* inflorescence meristems expressing *pWUS::3xVENUS-N7* (N_{WT}=94 flowers, $N_{vip3\text{-}1}$=58 flowers) and *pAG::AG-2xVENUS* (N_{WT}=54 flowers, $N_{vip3\text{-}1}$=41 flowers) reporters, labeled with FM4-64. Scale bars : 50 µm. (B) Histograms displaying the area of *pWUS ::3xVENUS-N7* (left) and *pAG::AG-2xVENUS*

(right) expression in the WT and *vip3-1* flowers of different size (<80 µm; 80 to 110 µm; >110 µm - flower diameter was calculated as described in Materials and methods). (C) Histograms displaying the average signal intensities for *pWUS ::3xVENUS-N7* (left) and *pAG::AG-2xVENUS* (right) in wild-type and *vip3-1* flowers of different size (<80 µm ; 80 to 110 µm ; >110 µm). The error bars represent the Standard error of mean, the results were considered significant when $\alpha \leq 0.05\%$ by two-tailed Student tests. (D) Graphical abstract: VIP3 contributes to the robustness of flower meristem termination.

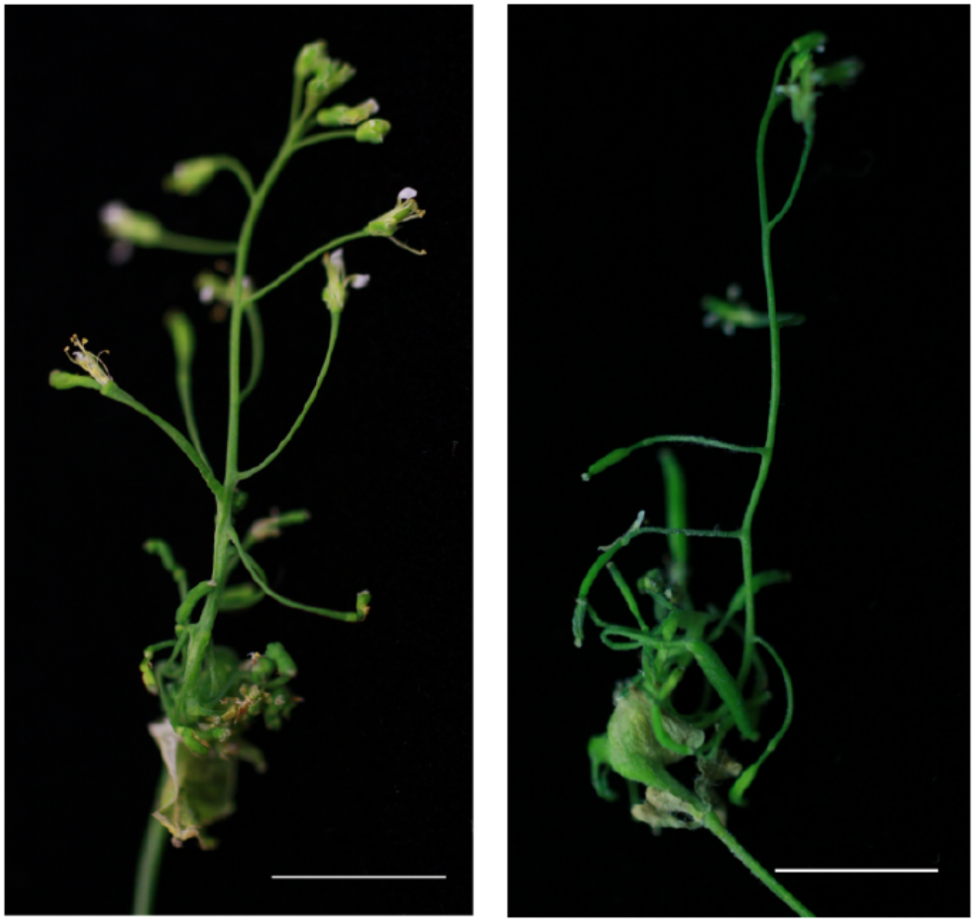

Fig. S1. Examples of the most severe indeterminacy phenotypes in *vip3-1* siliques.
Representative images of the most severe phenotypes in *vip3-1* flowers, displaying an inflorescence stem with siliques and flowers, emerging from a silique. Scale bar: 1 cm.

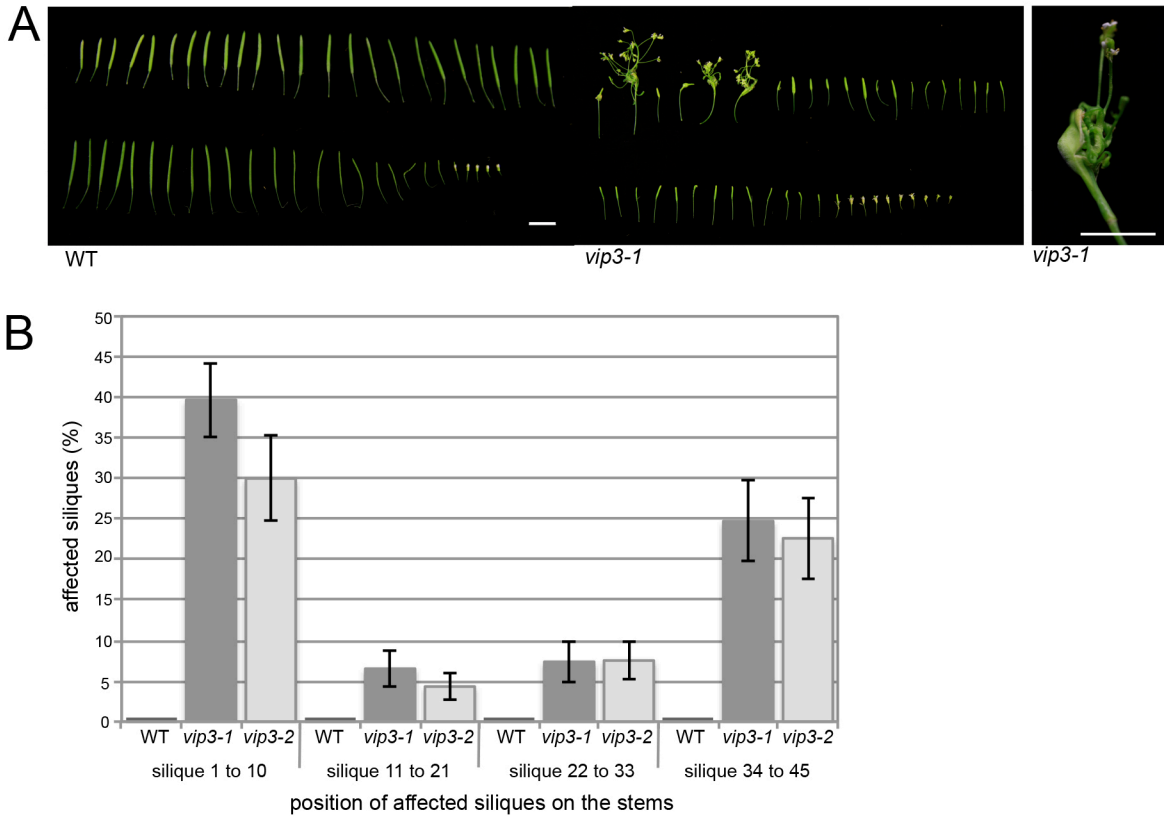

Fig. S2. *vip3* phenotype in short day then continuous light 21°C.

(A) Phenotype of WT (left panel) and *vip3-1* (middle panel) siliques, from plants grown in short day 21°C followed by continuous light 21°C conditions, harvested in a sequence of initiation along the stem. Scale bar : 1 cm. Right panel shows representative silique of the *vip3* displaying the indeterminacy phenotype. Scale bar : 5 mm. (B) Distribution (%) of affected siliques along the stems of the wild type (N=13), *vip3-1* (N=32) and *vip3-2* (N=21) grown in short day 21°C followed by continuous light 21°C condition (on average, 19% of *vip3-1* and 17% of *vip3-2* siliques displayed visible indeterminacy defects in these conditions).

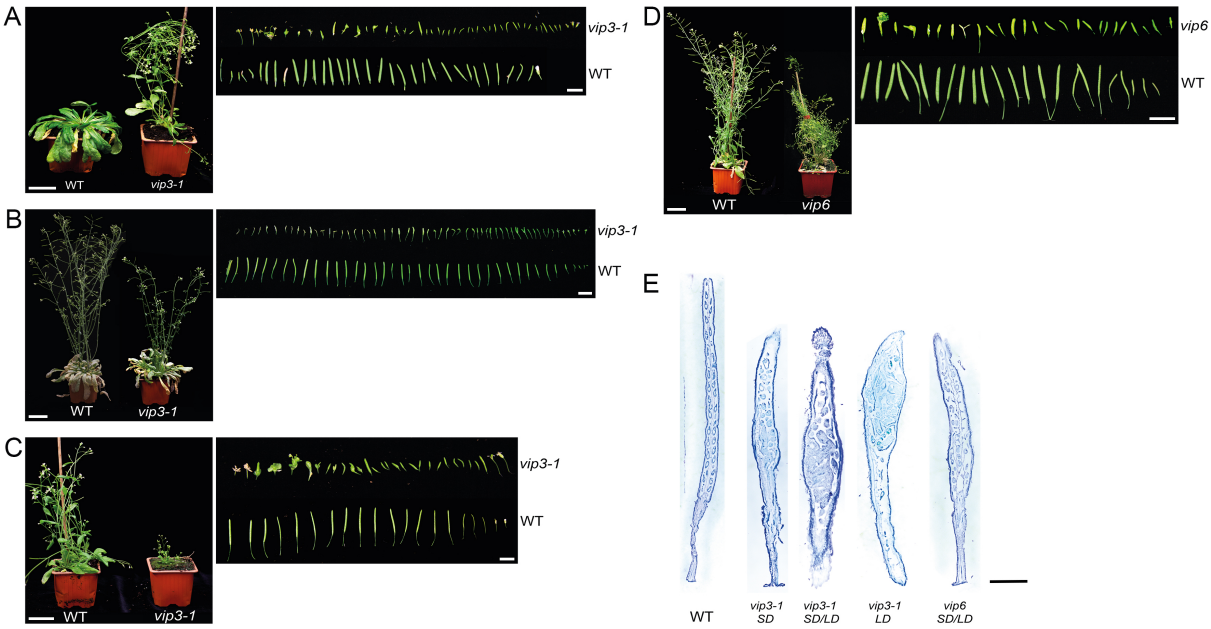

Fig. S3. Indeterminacy phenotype in different growth conditions and in different mutants of the Paf1 complex.

(A-C) Phenotypes of WT and *vip3-1* mutants grown in short day conditions (A, N=9 plants), in short then long day conditions (B, N=22 plants), and in long day conditions (C, N=22 plants). (D) Phenotype of WT and *vip6* mutant grown in short day 21°C followed by continuous light 16°C conditions displaying the indeterminacy phenotype (N=19 plants). For each condition, left panels display wild-type and *vip* adult plants, and right panels the siliques harvested in the order of their initiation along the stem. (E) Representative sections in young siliques, stained with toluidine blue, of *vip3-1*, in each culture condition, and *vip6* mutant, displaying the indeterminacy phenotype. Scale bars : 3 cm (A-D, left panels); 1 cm (A-D, right panels); 500 µm (E).

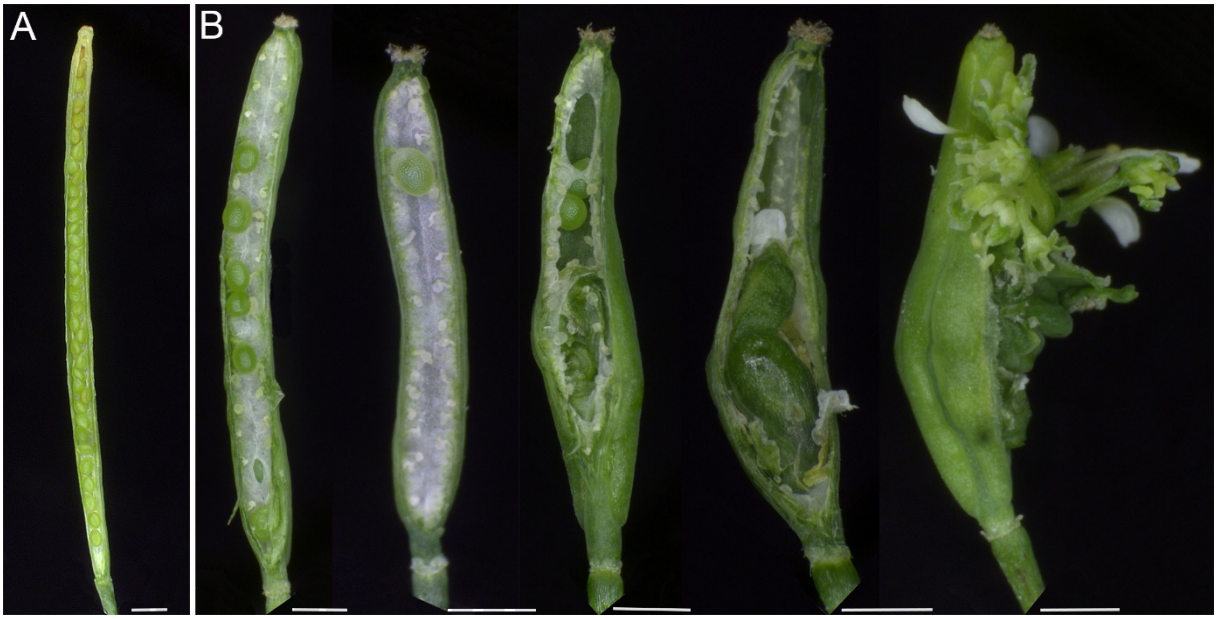

C	Number of ovules per silique		Number of aborted ovules per silique		Number of fertilized ovules per silique	
	WT	vip3-1	WT	vip3-1	WT	vip3-1
Mean	69,4	74,3	2,8	19,7	64,6	6,1
Standard deviation	3,9	18,2	0,9	11	3,7	6,8
Standard error of the mean	0,5	2,1	0,1	1,3	0,4	0,8
% compare to the total number of ovules per silique	-	-	4	26,5	93,1	8,2

Fig. S4. Proportion of aborted ovules and seeds in *vip3-1*.

(A-B) illustrates the range of phenotypes observed in *vip3-1* (B) compared to Col0 (A) (grown in short day and then in continuous light 16°C). *vip3-1* displays a strong and highly variable reduction of seed set in siliques showing no indeterminacy. In silique showing indeterminacy no or very few seeds usually develop. Bars = 500 µm. (C) Number of aborted ovules and seeds in *vip3-1* (N=73 siliques) and WT (N=70 siliques). The standard deviation reflects the variability of the original distribution. The standard error of the mean indicates the precision of estimated means (95% confidence interval).

A

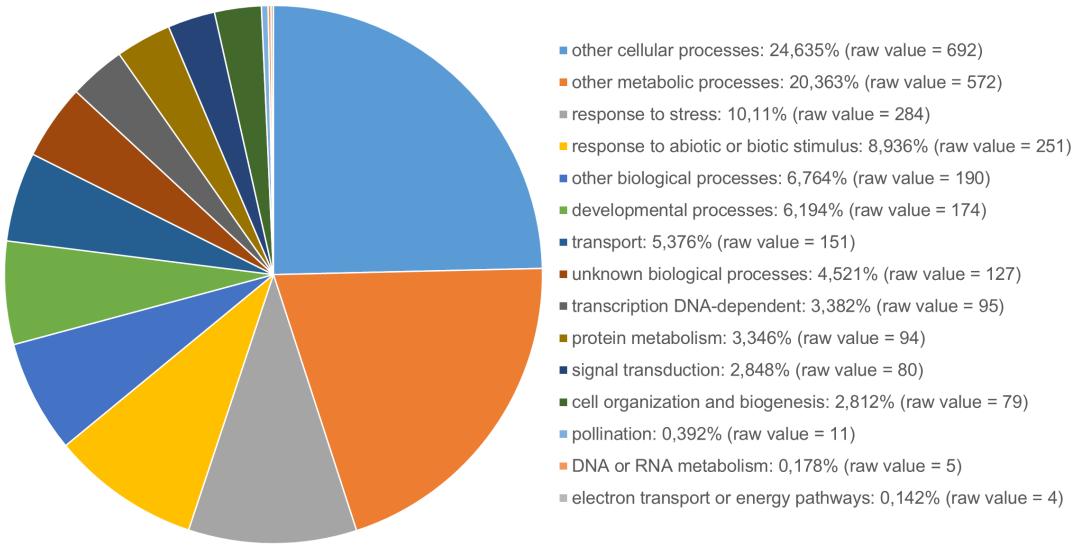

B

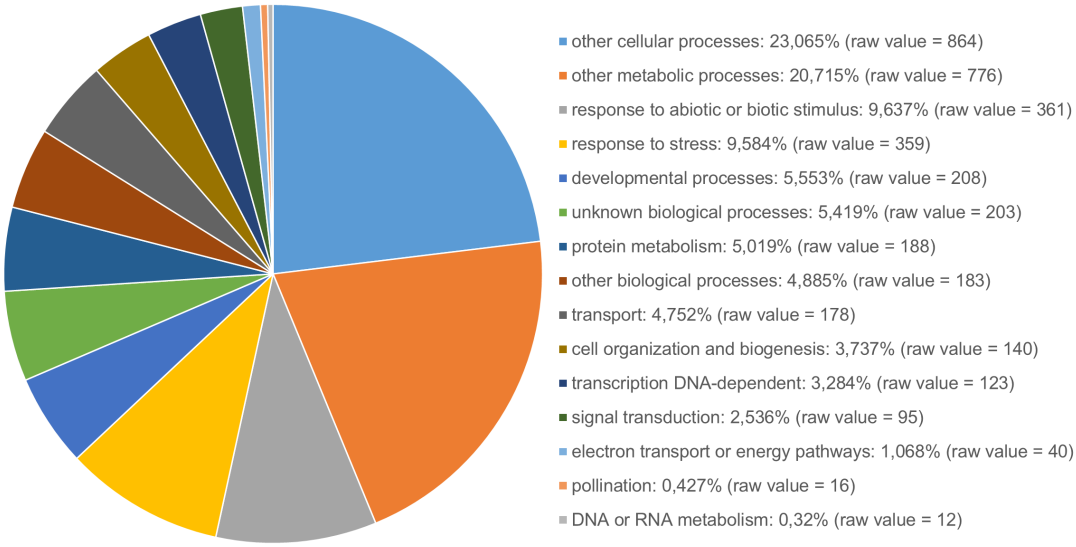

C

	gene_id	gene	log2(fold_change)	p_value
Downregulated	AT1G77080	FLM, FLOWERING LOCUS M / MAF1, MADS AFFECTING FLOWERING 1	-8,89394	5,00E-05
	AT5G65060	FCL3, FLOWERING LOCUS 3 / MAF3, MADS AFFECTING FLOWERING 3	-8,38456	0,0018
	AT5G10140	FLC, FLOWERING LOCUS C	-4,65699	5,00E-05
	AT5G65080	AGL68, AGAMOUS-LIKE 68 / MAF5, MADS AFFECTING FLOWERING 5	-4,15656	5,00E-05
	AT5G65050	AGL31, AGAMOUS-LIKE 31 / MAF2, MADS AFFECTING FLOWERING 2	-3,93607	5,00E-05
	AT5G38740	AGL77, AGAMOUS-LIKE 77	-3,33443	5,00E-05
	AT2G20825	ULT2, ULTRAPETALA2	-3,10298	5,00E-05
	AT5G27580	AGL89, AGAMOUS-LIKE 89	-2,67671	0,00405
	AT4G24540	AGL24, AGAMOUS-LIKE 24	-2,29325	5,00E-05
	AT4G27330	NZZ, NOZZLE / SPL, SPOROCYTELESS	-1,86166	0,00155
	AT5G60440	AGL62, AGAMOUS-LIKE 62	-1,59424	0,00795
	AT5G21150	AGO9, ARGONAUTE 9	-1,2134	5,00E-05
	AT5G57390	AIL5, AINTEGUMENTA-LIKE 5 / CHO1, CHOTTO 1 / EMK, EMBRYOMAKER / PLT5, PLETHORA 5	-0,866008	5,00E-05
	AT2G03060	AGL30, AGAMOUS-LIKE 30	-0,794353	0,001
	AT2G26440	PME12, PECTIN METHYLESTERASE 12	-0,709637	5,00E-05
Upregulated	AT3G20810	JMJ30 / JMJD5, JUMONJI DOMAIN CONTAINING 5	0,505522	0,00085
	AT4G37650	SGR7, SHOOT GRAVITROPISM 7 / SHR, SHORT ROOT	0,507952	0,00035
	AT2G33880	WOX9, WUSCHEL-RELATED HOMEOBOX 9	0,571996	0,00045
	AT2G34710	PHB, PHABULOSA / ATHB-14, ARABIDOPSIS THALIANA HOMEOBOX PROTEIN 14	0,586075	5,00E-05
	AT1G62360	STM, SHOOTMERISTEMLESS	0,589834	0,0001
	AT1G19850	MP, MONOPTEROS / ARF5, AUXIN RESPONSE FACTOR 5	0,608684	0,0019
	AT3G11050	FER2,- FERRITIN 2	0,652661	0,0039
	AT1G69770	CMT3, CHROMOMETHYLASE 3	0,707429	5,00E-05
	AT4G20270	BAM3, BARELY ANY MERISTEM 3	0,779995	5,00E-05
	AT5G62230	ERL1, ERECTA-LIKE 1	0,835578	5,00E-05
	AT5G53950	CUC2, CUP-SHAPED COTYLEDON 2	0,910426	5,00E-05
	AT5G11320	YUC4, YUCCA4	1,05308	5,00E-05
	AT2G45660	SOC1, SUPPRESSOR OF OVEREXPRESSION OF CO 1	1,0598	5,00E-05
	AT4G00150	HAM3, HAIRY MERISTEM 3, ATHAM3, HAIRY MERISTEM 3, HAM3, LOM3, LOST MERISTEMS 3, SCL6-IV	1,08428	5,00E-05
	AT1G68640	PAN; PERIANTHIA, TGA8, TGACG SEQUENCE-SPECIFIC BINDING PROTEIN 8	1,10476	5,00E-05
	AT3G15400	ATA20, ANTHER 20	2,05576	5,00E-05
	AT2G27250	CLV3, CLAVATA3	2,39061	5,00E-05
	AT1G75940	ATA27, BETA GLUCOSIDASE 20, BGLU20	2,50951	5,00E-05
	AT5G51870	AGL71, AGAMOUS-LIKE 71	2,85072	5,00E-05
	AT4G28395	ATA7, ARABIDOPSIS THALIANA ANTHER 7	3,11384	5,00E-05

D

	gene_id	gene	log2(fold_change)	p_value
Downregulated	AT2G14610	PR1; pathogenesis-related protein 1	-5,18392	5,00E-05
	AT5G59220	HAI1; PP2C protein (Clade A protein phosphatases type 2C)	-1,72227	5,00E-05
	AT4G34760	SAUR-like auxin-responsive protein family	-1,13968	5,00E-05
	AT1G08320	TGA9; bZIP transcription factor family protein	-0,969944	0,00355
	AT1G67710	ARR11; response regulator 11	-0,934393	0,00065
	AT3G23030	IAA2; indole-3-acetic acid inducible 2	-0,884945	0,0009
	AT4G34000	ABF3; abscisic acid responsive elements-binding factor 3	-0,857165	5,00E-05
	AT5G54510	DFL1; Auxin-responsive GH3 family protein	-0,799458	5,00E-05
	AT5G57560	TCH4; Xyloglucan endotransglucosylase/hydrolase family protein	-0,672642	5,00E-05
	AT3G23050	IAA7; indole-3-acetic acid 7	-0,628497	0,00325
	AT1G03430	AHP5; histidine-containing phosphotransfer factor 5	-0,590316	0,0007
	AT4G34750	SAUR-like auxin-responsive protein family	-0,579414	0,00535
Upregulated	AT1G80100	AHP6; histidine phosphotransfer protein 6	0,514231	0,0006
	AT2G22670	IAA8; indoleacetic acid-induced protein 8	0,537947	0,00075
	AT3G63010	GID1B; alpha/beta-Hydrolases superfamily protein	0,572849	0,00025
	AT1G28130	GH3.17; Auxin-responsive GH3 family protein	0,575311	5,00E-05
	AT5G46570	BSK2; BR-signaling kinase 2	0,576718	5,00E-05
	AT1G19850	MP; Transcriptional factor B3 family protein / auxin-responsive factor AUX/IAA-like protein	0,608684	0,0019
	AT1G51950	IAA18; indole-3-acetic acid inducible 18	0,628133	5,00E-05
	AT5G46790	PYL1; PYR1-like 1	0,646811	5,00E-05
	AT2G38120	AUX1; Transmembrane amino acid transporter family protein	0,691917	5,00E-05
	AT2G01570	RGA1; GRAS family transcription factor family protein	0,759926	5,00E-05
	AT1G45249	ABF2; abscisic acid responsive elements-binding factor 2	0,794846	5,00E-05
	AT1G19050	ARR7; response regulator 7	0,811842	5,00E-05
	AT2G38310	PYL4; PYR1-like 4	0,856148	5,00E-05
	AT4G27260	WES1; Auxin-responsive GH3 family protein	0,864813	5,00E-05
	AT1G72450	JAZ6; jasmonate-zim-domain protein 6	0,885443	5,00E-05
	AT1G17380	JAZ5; jasmonate-zim-domain protein 5	0,960683	5,00E-05
	AT4G33950	OST1; Protein kinase superfamily protein	1,02011	5,00E-05
	AT5G13220	JAZ10; jasmonate-zim-domain protein 10	1,03421	5,00E-05
	AT1G19180	JAZ1; jasmonate-zim-domain protein 1	1,04499	5,00E-05
	AT5G11320	YUC4, YUCCA4	1,05308	5,00E-05
	AT2G41310	RR3; response regulator 3	1,11732	5,00E-05
	AT1G77920	TGA7; bZIP transcription factor family protein	1,15091	0,00385
	AT5G17490	RGL3; RGA-like protein 3	1,15216	5,00E-05
	AT3G11410	PP2CA; protein phosphatase 2CA	1,21844	5,00E-05
	AT4G14550	IAA14; indole-3-acetic acid inducible 14	1,31153	0,0009
	AT1G04250	AXR3; AUX/IAA transcriptional regulator family protein	1,58048	0,0001
	AT3G21510	AHP1; histidine-containing phosphotransmitter 1	1,80767	0,00015
	AT1G77690	LAX3; like AUX1 3	2,1705	5,00E-05
	AT4G00880	SAUR-like auxin-responsive protein family	2,62316	5,00E-05
	AT5G13380	Auxin-responsive GH3 family protein	3,54665	5,00E-05
	AT2G46690	SAUR-like auxin-responsive protein family	3,63345	5,00E-05

Fig. S5. Differential gene expression in *vip3-1* vs. wild-type shoot apices.

(A, B) Gene ontology analysis: categories of genes involved in biological processes that are up-regulated (A) and down-regulated (B) in *vip3-1*. (C, D) Short list of genes involved in flowering and flower development (C) and signaling (D) pathways that are misexpressed in *vip3-1*. Genes that are down-regulated are highlighted in blue, and those that are up-regulated are highlighted in orange.

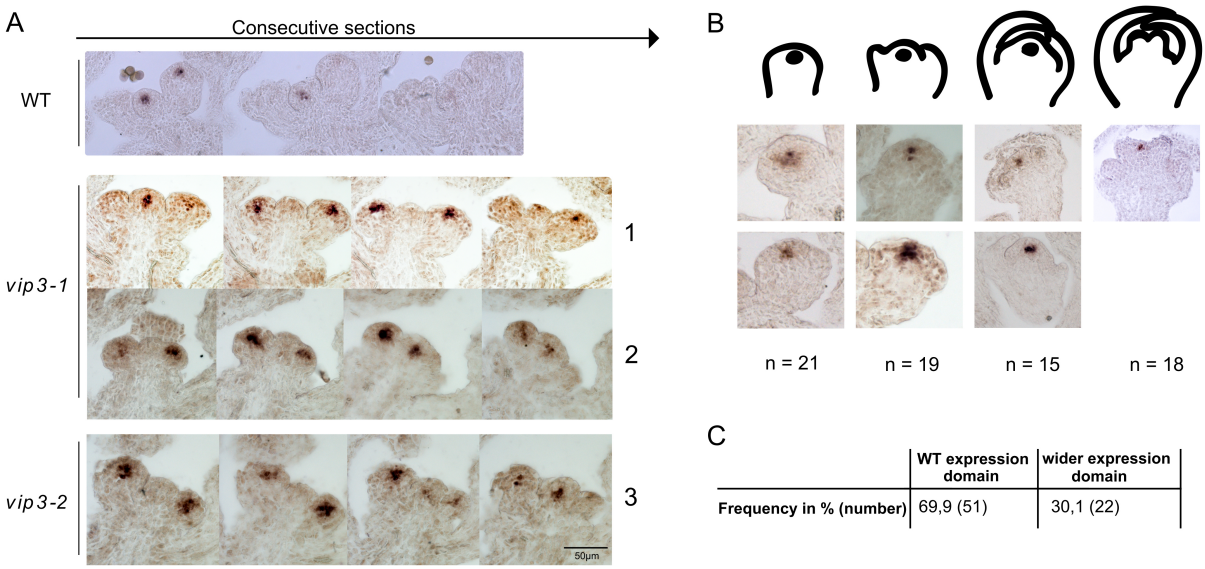

C

	WT expression domain	wider expression domain
Frequency in % (number)	69,9 (51)	30,1 (22)

Fig. S6. Expression patterns of *WUS* in *vip3* flowers.

(A, B) *In situ* hybridization of *WUS* transcripts in wild-type (A, upper panel) and *vip3-1* (A, lower panel and B). (A) Consecutive sections on WT and 3 independent *vip3* (1-2: *vip3-1*; 3: *vip3-2*) apices showing an expansion of *WUS* expression domain in *vip3-1* floral meristems, when compared to wild type. (B) Representative patterns of *WUS* expression domain in *vip3-1* flower buds at four different developmental stages (as represented by schematic drawings). Plants were grown in short day then continuous light 16°C conditions (as in Fig. 1). Scale bar: 50 µm. (C) Number of flower meristems displaying a wild-type *WUS* expression domain and an enlarged *WUS* expression domain in *vip3-1*.

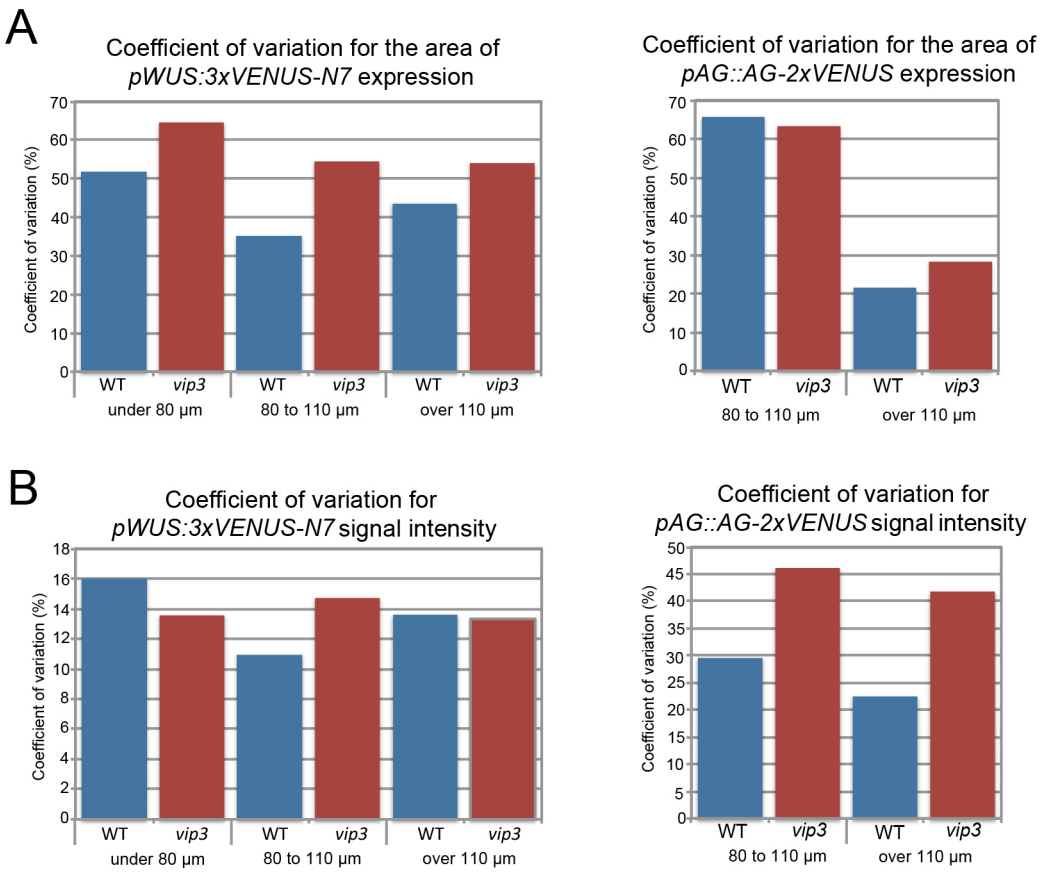

Fig. S7. Coefficient of variation for *WUS* and *AG* expression area and average intensity in *vip3* flowers

(A) Histograms displaying the coefficients of variation (%) for the area of *pWUS::3xVENUS-N7* (left) and *pAG::AG-2xVENUS* (right) expression in wild-type and *vip3-1* flowers. (B) Histograms displaying the coefficients of variation for the average fluorescence signal intensity of *pWUS::3xVENUS-N7* (left) and *pAG::AG-2xVENUS* (right) expression in wild-type and *vip3-1* flowers.

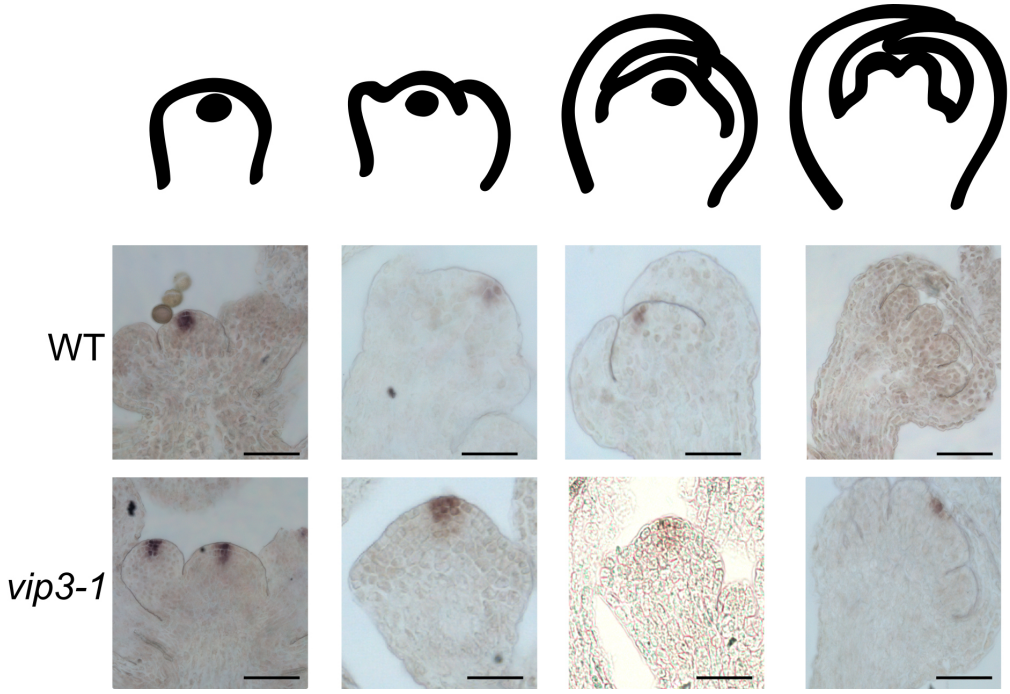

Figure S8. Expression patterns of *CLV3* in *vip3-1* flowers

In situ hybridization of *CLV3* transcripts in wild-type (A) and *vip3-1* (B). Plants were grown in short day then continuous light 16°C conditions (as in Figure 1). Scale bar = 50 µm.

Table S1. List of primers

Name	Sequence
Genotyping primers	
LBb1.3	ATTTTGCCGATTTCGGAAC
vip3-1 F	GACTGCAAGTACCACTTTCGC
vip3-1 R	TAATGGGAAACGACTTGCTTG
vip3-2 F	CTGACTGGATCTCTTGACGAGACG
vip3-2 R	GATACTCAGCAATTCCATATAGTACCCAAGC
Primers for *in situ* probes	
*WUS_in_situ*_F	CAACAAGTCCGGCTCTGGTG
*WUS_in_situ*_RT7	TGTAATACGACTCACTATAGGGCGGGAAGAGAGGAAGCGTACGTCG
*AG_in_situ*_F	ACGGCGTACCAATCGGAGCT
*AG_in _situ*_RT7	TGTAATACGACTCACTATAGGGCGTTGCAATGCCGCGACTTGG
CLV3_in_situ_F	ATGTCCGGTCCAGTTCAACAAC
CLV3_in_situ_RT7	TGTAATACGACTCACTATAGGGCGGTCAGGTCCCGAAGGAACA
Primers for *pAG::AG-2xVenus* construction	
pPD381	GTCCCCGGGAGTGATCCCTTCTCCAACACA
pPD413	AGTCCCGGGTAACTGGAGAGCGGTTTGGT
pPD441	AGTGGATCCGCAGCTGCCGCAGCTGCGATGGTGAGCAAGGGCGAG
pPD442	GTCTCTAGACTAGATAGATCTCTTGTACAGCTC